CHEMPHYSCHEM

DOI: 10.1002/cphc.201000034

Generation of Highly Damaging H_2O^+ Radicals by Inner Valence Shell Ionization of Water

Oriol Vendrell,* Spas D. Stoychev, and Lorenz S. Cederbaum*[a]

Water molecules surround all biological matter and have a crucial role as the matrix of life. Owing to the close proximity of water molecules to all biological systems, it is important to understand the response of water to ionizing sources, since the emitted electrons and open-shell fragments play a major role in various damaging mechanisms of biomolecules. Very recent experiments have investigated the inner valence ionization of water in the water dimer[1] and in larger water clusters,[2] and have found that the system decays emitting electrons of low energy and radical cations H_2O^+. Low-energy electrons can effectively interact and induce breakage of biomolecules. The water radical cation is also capable of great damage.[3,4] It is a strong acid and will immediately transfer a proton to any nearby group with proton-accepting capability. The proton transfer results in $OH^•$, which is extremely reactive itself. In nature and experimentally the inner valence ionization can be accomplished by interaction with light. Other preparations are also conceivable, for example, an inner-valence ionized state can be the result of a cascade of processes, such as Auger decay, started by ionization or excitation of a core electron by an energetic particle or photon. The process by which an inner-valence ionized state decays by emission of an electron is called intermolecular Coulombic decay (ICD). ICD is an electronic deexcitation process that was first theoretically predicted for hydrogen-bonded systems[5,6] and van der Waals clusters of noble gas atoms.[7] Later, experimental evidence of ICD in van der Waals clusters was reported,[8,9] and more recently, evidence of ICD in water has been reported as well.[1,2,10] ICD can take place if the inner valence ionized state is energetically above the double-ionization threshold of the system. This is usually not the case for isolated atoms or small molecules. However, for aggregates, the double ionization threshold can fall below the inner valence ionization energy, opening the possibility for ICD to occur. The process can be described as a relaxation of the ionized atom or molecule, in which an outer valence electron fills the inner valence hole. The energy released is transferred to a neighboring species, from which a second outer valence electron is expelled. In the case of the water dimer, the double ionization threshold is about 3 to 4 eV below the inner valence ionization energy, and therefore ICD follows an inner valence ionization process.[6]

In the experiments on the water dimer of ref. [1], the ICD process is triggered by ionization from an inner valence shell of one of the water molecules. The two emitted electrons (direct photo-electron and ICD electron) and the cationic fragments resulting from the Coulomb explosion of the dimer are then measured in coincidence, determining their directions, and the charges and masses of the fragments. Such experiments clearly show that ICD results in two H_2O^+ fragments, which immediately separate in a Coulomb explosion. Other scenarios could in principle be conceived, such as an ultrafast proton transfer from the hydrogen-bond donor to the hydrogen-bond acceptor molecule while the system is still in a singly ionized state,[11] followed by ICD and Coulomb explosion of the H_3O^+ and OH^+ fragments. However, this decay channel is not observed experimentally, supporting the notion that in fact ICD is a very fast process in water. ICD in water can have far-reaching consequences for the damage to biological structures. An ICD event not only generates two H_2O^+, additionally they are generated as neighbour ions, which leads to an immediate release of Coulomb repulsion energy, of the order of 5 eV, as translational, rotational, and vibrational energy of the fragments. The sum of the translational kinetic energies (kinetic energy release, KER) of the repelling H_2O^+ fragments is reported from the experiments, but nothing is known about the internal state of the two water radical cations after the Coulomb explosion. The KER can easily be estimated as the potential energy of two positive charges at the equilibrium oxygen–oxygen distance of the water dimer, which is 2.9 Å. This simple estimation leads to an expected KER of about 4.9 eV. However, the experimental KER distribution lies clearly below this value, suggesting that a considerable amount of energy ends up trapped in the vibrational and rotational degrees of freedom of the H_2O^+ fragments.

Herein, we simulate the Coulomb explosion of the ionized water dimer by ab initio molecular dynamics (AIMD), giving a detailed picture of the mechanism by which two water radical cations separate after inner valence ionization followed by ICD, and how the energy is distributed among the rotational and vibrational degrees of freedom of the fragments after the explosion. The computed probability distribution of the KER of the H_2O^+ fragments is compared to the experimental results of ref. [1]. Observable quantities are computed quasi-classically from averaging over 1500 classical trajectories. Averaged quantities over all trajectories are denoted as $\langle\Lambda\rangle$ throughout. The initial positions and velocities of each trajectory are sampled from the Wigner distribution of the quantum-mechanical vibrational ground state of the neutral dimer in harmonic approxi-

[a] Dr. O. Vendrell, S. D. Stoychev, Prof. L. S. Cederbaum
Theoretische Chemie
Physikalisch-Chemisches Institut, Universität Heidelberg
Im Neuenheimer Feld 229, 69120 Heidelberg (Germany)
Fax: (+49)-6221-54-5215
E-mail: oriol.vendrell@pci.uni-heidelberg.de
lorenz.cederbaum@pci.uni-heidelberg.de

Supporting information for this article is available on the WWW under http://dx.doi.org/10.1002/cphc.201000034.

mation. Each trajectory is numerically integrated on the potential energy surface (PES) of the ground electronic state of the dication, computed at the second-order Møller–Pleset perturbation theory. The trajectory integrations were performed using the Gaussian 03 program package.[12] Further details on the trajectory integrations are provided in the Supporting Information.

Figure 1a shows the calculated average KER as a function of time. Its value approaches an asymptotic limit, but it would require extremely long propagations to reach the true asymptote of ⟨KER⟩ due to the long range of the Coulomb interaction. However, such long propagations are not necessary, because at large distances both fragments already see each other as point charges (i.e. any interaction except for the Coulomb one is negligible). The KER value for each single trajectory is then obtained by adding the Coulomb energy corresponding to the distance between both fragments at $t=800$ fs to the KER resulting from the trajectory propagation. The corrected KER (c-KER), shown in Figure 1b, takes into account the internal and rotational dynamics of the fragments, and has the correct asymptotic behaviour. On the other hand, the initial-conditions KER (i-KER) distribution is computed from the distance between both oxygens at $t=0$ fs, and completely neglects any internal and rotational dynamics of the H_2O^+ cations as they fall apart, therefore assuming that the Coulomb potential energy is entirely released as translational kinetic energy of the fragments. The maximum of the experimental KER distribution is located at 4.2 eV, and compares well with the maximum of the c-KER distribution, which is 4.3 eV. For both distributions, the probability of a KER of 4.9 eV is low. However, the experimental distribution extends to lower energies, which is probably related to the nuclear dynamics of the singly-ionized system after photo-ionization, and before the onset of ICD. The lack of quantum effects in our simulations, the harmonic approximation of the ground vibrational state of the dimer used to sample the initial conditions, and the experimental accuracy, might also play a role in the deviations between the computed c-KER and experiment. Conversely, the i-KER is precisely centered at 5.0 eV and has little overlap with the experimental KER. The i-KER is shifted 0.6 to 0.8 eV to higher energies with respect to the c-KER distribution, illustrating the fact that rotational and internal degrees of freedom of the H_2O^+ fragments absorb an important amount of energy during the Coulomb explosion.

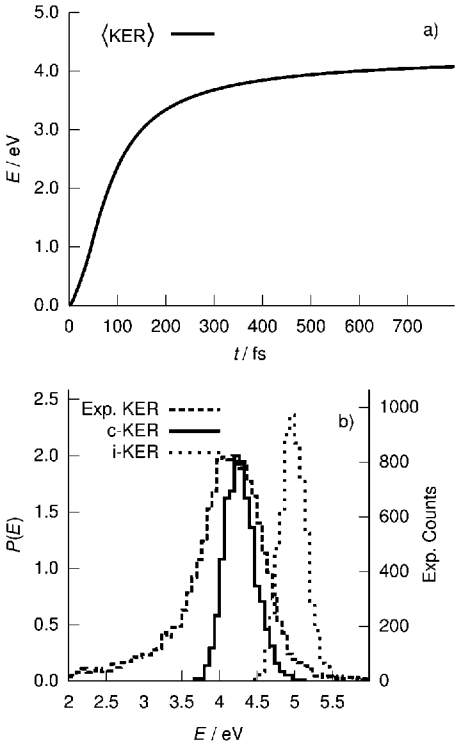

Figure 1. a) Computed average ⟨KER⟩ as a function of time. b) Experimental and simulated KER distributions. For the experiment, the number of counts at a given energy as reported in Ref.[1] is given. c-KER refers to the KER computed from the system dynamics with asymptotic correction, while i-KER is the KER obtained solely from the distance between the oxygen atoms at $t=0$ fs. The left *y*-axis represents a probability density for a total probability of 1.

Figure 2a shows the average rotational energy, and the kinetic energy of the internal vibrations of each fragment along time. Details on the calculation of these quantities are given as Supporting Information. The curves do not start at zero energy for $t=0$, because the initial conditions are sampled from a Wigner distribution of the water dimer. The average energy released into vibrations and rotations corresponds to the differ-

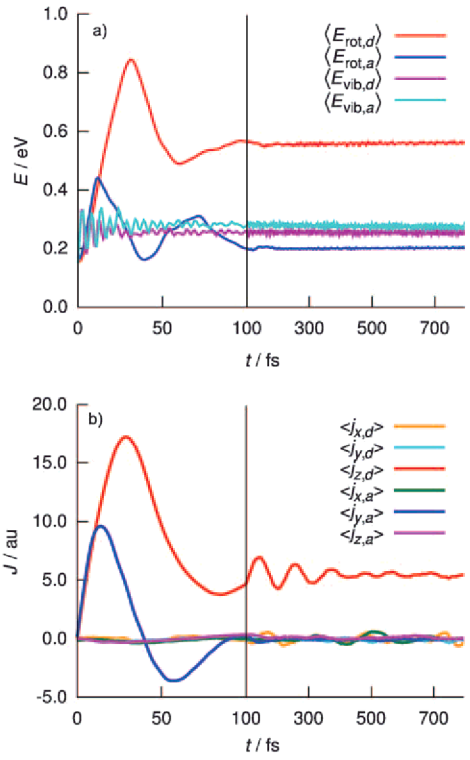

Figure 2. a) Average rotational and vibrational energies of the donor and acceptor H_2O^+ fragments as a function of time. b) Average components of the total angular momentum of each fragment projected onto molecule-fix axes. The definition of the axes is given in the text. The vertical line denotes a change of timescale.

ence between the values at $t=800$ fs, which have long since reached their asymptotic behaviour, and the values at $t=0$ fs, which reflect the initial energy distribution. The average increment of internal and rotational energy of both fragments is 0.65 eV. Of these, 0.41 eV correspond to rotational energy of the donor, 0.09 eV to vibrational energy of the donor, 0.04 eV to rotational energy of the acceptor, and 0.11 eV to vibrational energy of the acceptor.

The rotational energies of both fragments oscillate strongly until they reach their final values after about 150 fs, when the two H_2O^+ are found at an average distance of about 11 Å. Until that point, there is exchange of translational and rotational energy between both fragments. After 30 fs the donor molecule reaches its maximum rotational energy of more than 0.8 eV. It can also be seen in Figure 2a that there is no rotation–vibration energy exchange, and that the vibrational energies oscillate from the beginning around their final asymptotic value.

Interestingly, more than half of the energy going into rotational and vibrational motion ends up as rotational energy of the hydrogen-bond donor molecule. In order to disentangle the rotational dynamics of each of the H_2O^+ fragments, the components of their angular momenta are computed on a set of molecule-fixed orthogonal axes x, y and z that have their origin in the center of mass (CM) of each molecule. For each water molecule, the x-axis connects the CM of the molecule with the CM of both hydrogens, and the z-axis is perpendicular to the plane of the molecule. The y-axis is then defined as perpendicular to x and z. The average values of the components of the angular momenta $\langle j_{x,w}\rangle$, $\langle j_{y,w}\rangle$, and $\langle j_{z,w}\rangle$ for each fragment are presented in Figure 2b, where $w=(d,a)$ for the donor and acceptor molecules, respectively. The details of the calculation of the angular momenta are given in the Supporting Information. Each component of the angular momentum can have either a positive or a negative sign depending on the sense of rotation around that particular axis. Due to the symmetry of the water dimer, $\langle j_{x,d}\rangle$ and $\langle j_{y,d}\rangle$ for the donor and $\langle j_{x,a}\rangle$ and $\langle j_{z,a}\rangle$ for the acceptor cancel at all times, although such components do not vanish in general for individual trajectories.

Figure 3 shows snapshots of the particular trajectory starting from the minimum energy geometry of the neutral dimer with zero initial kinetic energy. This trajectory illustrates the average behaviour during the explosion. Initially, the donor molecule starts to rotate strongly around its z-axis, performing full turns. This is seen clearly in Figure 2b, where $\langle j_{z,d}\rangle$ never changes sign. At the same time, the acceptor molecule starts a hindered rotation around its y-axis in a well defined sense of rotation. The acceptor does not have enough rotational energy to perform full turns, which are hindered by the interaction with the donor molecule. This is seen in the changes of sign of $\langle j_{y,a}\rangle$ with time. Finally, $\langle j_{y,a}\rangle$ tends to zero, indicating that when the molecules are freely rotating at large distances, all memory of the direction in which the initial impulse was given to the acceptor molecule has been lost. Only $\langle j_{z,d}\rangle$ retains an asymptotic value different from zero.

In conclusion, we report a detailed picture of the events after an inner valence ionization of the water dimer followed by ICD decay. Very recent experiments have shown that this is *the* decay channel in water after inner valence ionization. After ICD, two neighbouring H_2O^+ fragments are generated, which quickly separate in a Coulomb explosion, gaining a large amount of translational and rotational energy. The internal and rotational dynamics of the fragments during the explosion is simulated, the distribution of kinetic energy of the generated H_2O^+ fragments is compared to the experiments, and good agreement is found. Experimentally, the final kinetic energy of the fragments is lower than the estimation obtained by considering the initial distance between the cations. Our simulations show that a non-negligible portion of the Coulomb repulsion energy ends up as rotational energy of the hydrogen-bond donor water molecule, accounting for the experimentally measured KER. The rotational energy of both H_2O^+ cations varies with an oscillating pattern until 150 fs after the Coulomb explosion, when they are about 11 Å apart. After this point, both cations gain only translational kinetic energy. The H_2O^+ fragment corresponding to the hydrogen-bond donor maintains its sense of rotation around the axis perpendicular to the molecular plane indefinitely, and its rotational energy after the explosion is of about 0.6 eV. Conversely, the fragment generating from the acceptor molecule has lost all information on the initial sense of rotation by the time the cations are freely rotating. The reported simulations assume an instantaneous ICD decay, neglecting the nuclear dynamics of the singly ionized cluster before the onset of ICD and the decay to the doubly-ionized state. The low-energy tail of the experimental KER in Figure 1b is most probably related to the vibrational dynamics effects of the singly ionized cluster during the first few femtoseconds after the photoionization, and such effects will be the subject of future investigations. The reported simulations present fundamental information on the dynamics of water after ionization by high energy sources, and our findings are important for understanding future experiments on electronic decay processes and ionization in water medium.

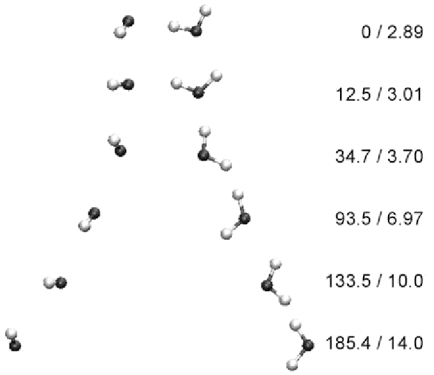

Figure 3. Side view of the Coulomb explosion starting from the minimum energy geometry of the water dimer and with zero initial kinetic energy. The numbers at the right side denote time in femtoseconds and oxygen-oxygen distance in Angstroms. For this particular trajectory, the y-axis of the acceptor molecule (left) and the z-axis of the donor molecule (right) are at all times perpendicular to the plane defined by the three atoms of the donor. The definition of the molecule-fix axes is found in the main text. The perspective is such that one of the hydrogen atoms of the acceptor is eclipsed by the other hydrogen atom at all times.

Acknowledgements

The research leading to these results has received funding from the European Research Council under the European Community's Seventh Framework Programme (FP7/2007-2013)/ERC Advanced Investigator Grant no. 227597. We thank Prof. Dörner for providing us with the experimental data and Prof. Hergenhahn for useful discussions.

Keywords: ab initio calculations · coulomb explosion · intermolecular coulombic decay · molecular dynamics · water chemistry

[1] T. Jahnke, H. Sann, T. Havermeier, K. Kreidi, C. Stuck, M. Meckel, M. Schöffler, N. Neumann, R. Wallauer, S. Voss, A. Czasch, O. Jagutzki, A. Malakzadeh, F. Afaneh, Th. Weber, H. Schmidt-Böcking, R. Dörner, *Nature Physics* **2010**, *6*, 139 – 142.

[2] M. Mucke, M. Braune, S. Barth, M. Förstel, T. Lischke, V. Ulrich, T. Arion, A. M. Bradshaw, U. Becker, U. Hergenhahn, *Nature Physics* **2010**, *6*, 143 – 146.

[3] P. O'Neill, D. L. Stevens, E. F. Garman, *J. Synchrotron Radiat.* **2002**, *9*, 329 – 332.

[4] S. Purkayastha, J. R. Milligan, W. A. Bernhard, *J. Phys. Chem. B* **2005**, *109*, 16967 – 16973.

[5] L. S. Cederbaum, J. Zobeley, F. Tarantelli, *Phys. Rev. Lett.* **1997**, *79*, 4778 – 4781.

[6] I. B. Müller, L. S. Cederbaum, *J. Chem. Phys.* **2006**, *125*, 204305.

[7] R. Santra, J. Zobeley, L. S. Cederbaum, N. Moiseyev, *Phys. Rev. Lett.* **2000**, *85*, 4490 – 4493.

[8] T. Jahnke, A. Czasch, M. S. Schöffler, S. Schössler, A. Knapp, M. Käsz, J. Titze, C. Wimmer, K. Kreidi, R. E. Grisenti, A. Staudte, O. Jagutzki, U. Hergenhahn, H. Schmidt-Böcking, R. Dörner, *Phys. Rev. Lett.* **2004**, *93*, 163401.

[9] G. Öhrwall, M. Tchaplyguine, M. Lundwall, R. Feifel, H. Bergersen, T. Rander, A. Lindblad, J. Schulz, S. Peredkov, S. Barth, S. Marburger, U. Hergenhahn, S. Svensson, O. Björneholm, *Phys. Rev. Lett.* **2004**, *93*, 173401.

[10] E. F. Aziz, N. Ottosson, M. Faubel, I. V. Hertel, B. Winter, *Nature* **2008**, *455*, 89 – 91.

[11] H. Tachikawa, *J. Phys. Chem. A* **2004**, *108*, 7853 – 7862.

[12] M. J. Frisch, G. W. Trucks, H. B. Schlegel, G. E. Scuseria, M. A. Robb, J. R. Cheeseman, J. A. Montgomery, Jr., T. Vreven, K. N. Kudin, J. C. Burant, J. M. Millam, S. S. Iyengar, J. Tomasi, V. Barone, B. Mennucci, M. Cossi, G. Scalmani, N. Rega, G. A. Petersson, H. Nakatsuji, M. Hada, M. Ehara, K. Toyota, R. Fukuda, J. Hasegawa, M. Ishida, T. Nakajima, Y. Honda, O. Kitao, H. Nakai, M. Klene, X. Li, J. E. Knox, H. P. Hratchian, J. B. Cross, V. Bakken, C. Adamo, J. Jaramillo, R. Gomperts, R. E. Stratmann, O. Yazyev, A. J. Austin, R. Cammi, C. Pomelli, J. W. Ochterski, P. Y. Ayala, K. Morokuma, G. A. Voth, P. Salvador, J. J. Dannenberg, V. G. Zakrzewski, S. Dapprich, A. D. Daniels, M. C. Strain, O. Farkas, D. K. Malick, A. D. Rabuck, K. Raghavachari, J. B. Foresman, J. V. Ortiz, Q. Cui, A. G. Baboul, S. Clifford, J. Cioslowski, B. B. Stefanov, G. Liu, A. Liashenko, P. Piskorz, I. Komaromi, R. L. Martin, D. J. Fox, T. Keith, M. A. Al-Laham, C. Y. Peng, A. Nanayakkara, M. Challacombe, P. M. W. Gill, B. Johnson, W. Chen, M. W. Wong, C. Gonzalez, J. A. Pople, *Gaussian 03, Revision C.02*, Gaussian, Inc., Wallingford CT, **2004**..

Received: January 18, 2010
Published online on February 9, 2010

